Influence of Long-Chain Branching on the Miscibility of Poly(ethylene-*r*-ethylethylene) Blends with Different Microstructures

YING YING CHEN,[1] TIMOTHY P. LODGE,[1,2] FRANK S. BATES[1]

[1]Department of Chemical Engineering and Materials Science, University of Minnesota, Minneapolis, Minnesota 55455
[2]Department of Chemistry, University of Minnesota, Minneapolis, Minnesota 55455

Received 25 June 2001; revised 20 November 2001; accepted 5 December 2001

ABSTRACT: The melt miscibility of two series of poly(ethylene-*r*-ethylethylene) (PE_{Exx}) polymers with different percentages (*xx*) of ethylethylene (EE) repeat units was examined with small-angle neutron scattering (SANS). The first series consisted of comb/linear blends in which the first component is a heavily branched comb polymer (B90) containing 90% EE and an average of 62 long branches with a weight-average molecular weight (M_W) of 5.5 kg/mol attached to a backbone with M_W = 10.0 kg/mol. The comb polymer was blended with six linear PE_{Exx} copolymers, all of which had $M_W \approx 60$ kg/mol and EE percentages ranging from 55 to 90%; they were denoted L55 to L90, with the number referring to the percentage of EE repeat units. The second series consisted of linear/linear blends; the first component, with M_W = 220 kg/mol and 90% EE, was denoted L90A, and the second components were the same series of linear polymers, with $M_W \approx 60$ kg/mol and various EE compositions. The concentrations investigated were 50/50 w/w, except for the blend of branched B90 and linear L90 (both components were 90% EE), for which 25/75 and 75/25 concentrations were also examined. The SANS results indicated that for the comb/linear blends, only the dB90/L90 blends were miscible, whereas the other five blends phase-separated; for the linear/linear blends, dL90A/L83 and dL90A/L78 were miscible, whereas the other three blends were immiscible. These results indicate that long-chain branching significantly narrowed the miscibility window of these polyolefin blends. © 2002 John Wiley & Sons, Inc. J Polym Sci Part B: Polym Phys 40: 466–477, 2002; DOI 10.1002/polb.10102

Keywords: polymer blends; branching; entropic χ parameter; small-angle neutron scattering (SANS); polyolefins; compatibility

INTRODUCTION

Molecular architecture is a major factor influencing polymer blend phase behavior. Long-chain branching in particular represents an architectural variable that can drastically effect the behavior of plastics, including melt rheology, crystallinity percentage, and other solid-state properties. It is especially important for polyolefins, a class of saturated hydrocarbons for which branching plays a key role in processing and product optimization and for which modern synthetic strategies of commercial importance lead directly to architectural variability.

Two of the most important polyolefins are low-density polyethylene (LDPE) and high-density polyethylene (HDPE). LDPE is characterized by a complex arrangement of long and short branches, whereas HDPE is essentially linear. The different properties of LDPE and HDPE render them use-

Correspondence to: Timothy P. Lodge (E-mail: lodge@chem.umn.edu)

Journal of Polymer Science: Part B: Polymer Physics, Vol. 40, 466–477 (2002)

ful in quite different applications. A significant controversy in this field centers on the issue of miscibility in LDPE and HDPE. Wignall and coworkers[1,2] studied a series of LDPE/HDPE blends employing small-angle neutron scattering (SANS). After accounting for the effects of isotopic substitution and crystallinity, they concluded that the mixtures were homogenous (one phase) for all compositions. Barham and coworkers[3–5] also investigated the miscibility of LDPE/HDPE blends, using differential scanning calorimetry (DSC) and transmission electron microscopy, and concluded that binary and ternary blends of HDPE and two different LDPE components phase-separated under certain conditions. Tsukahara et al.'s work[6] on branched and linear polystyrene blends indicated phase separation at high branching densities according to DSC measurements, whereas Greenberg and coworkers[7,8] deduced miscibility for blends of star and linear polystyrene from SANS experiments.

Although a variety of theoretical approaches have been developed to account for the thermodynamics of mixed polymer blends (these include the solubility parameter,[9–13] lattice cluster theory,[14–17] polymer reference interaction site model,[18–20] and field theory[21–25]), only field theory directly predicts the effect of long-chain branching on polyolefin blend miscibility in a relatively straightforward way. The field theory is developed from the random phase approximation (RPA) and Flory–Huggins theories, in which the focus is on the importance of the excess entropy arising from long-range, nonlocal effects.

To better understand the effect of branching on polyolefin blend miscibility, we examined the influence of long-chain branching experimentally with highly branched, comblike model polyolefins and their linear counterparts. In a previous report,[26] we investigated by SANS the phase behavior of comb/linear polymer blends in which the only difference between the two components was the architecture. The results established that the entropic contribution to the excess free energy due to architectural effects was the major contributor and further demonstrated that architectural asymmetry alone was sufficient to induce phase separation in these otherwise nearly ideal mixtures. The data agreed qualitatively with the predictions of field theory, indicating that the theory is a promising guide for understanding the thermodynamic phase behavior of long-chain-branched/linear polyolefin blends.

To further explore the thermodynamics of long-chain-branched/linear polyolefin blends, in this study we introduced another important contribution to the excess free energy, namely, the heat of mixing. We investigated two series of polyolefin blends, in which either a comb polymer or a linear polymer was mixed with linear polymers of different microstructures. With linear/linear blends, the main factor that influences the miscibility is the microstructure difference, as thoroughly documented by Graessley and coworkers.[9–13] However, for the comb/linear blends, there will be two effects in competition: long-chain branching, an entropic contribution, and the microstructure difference, largely an enthalpic contribution. In comparing the results of these two series of blends, we can develop a better understanding of how long-chain branching affects blend miscibility.

The poly(ethylene-*r*-ethylethylene) polymer system is designated PE_{Exx}, a random copolymer containing molar percentages of $(100 - xx)$ ethylene and *xx* ethylethylene (EE) repeat units. An advantage of this system is that the percentage of EE can be tuned gradually, providing an increasingly different microstructure.

EXPERIMENTAL

Anionic Polymerization

Linear Polybutadienes

Seven linear polybutadiene samples were synthesized with standard anionic polymerization techniques.[27,28] The initiator was *sec*-butyllithium (Aldrich), and the reactions were carried out at different temperatures in a mixture of cyclohexane (American Chemical Society; Aldrich) and tetrahydrofuran (THF; ACS; Aldrich) at different [THF]/[Li] ratios. These conditions led to different levels of 1,2-addition as determined by solution ^{1}H NMR spectroscopy. Termination was accomplished with degassed isopropanol. The detailed synthesis conditions are listed in Table 1. These linear polymers are denoted L*xx*, where L and *xx* refer to the linear architecture and percentage of EE repeat units in the polymer, respectively.

Highly Branched Polybutadienes

The backbone precursor polymer was synthesized with the same technique as the linear polybutadienes, but at a [THF]/[Li] ratio of 4/1 and a reaction temperature of 20 °C. The resulting de-

Table I. Synthesis Conditions for Varying Micro-structured Linear Polybutadienes

Polymer	Temperature (°C)	[THF]:[I] Ratio	Reaction Time (hr)	1,2 Addition[a]
L90A	0	150:1	18	90%
L90	0	150:1	18	90%
L83	12	120:1	18	83%
L78	16	100:1	24	77%
L73	20	85:1	24	73%
L68	25	75:1	24	68%
L55	40	55:1	18	55%
B90	0	150:1	18	90%

[a] Based on ^{1}H NMR.

gree of 1,2-addition was determined to be 67% by solution ^{1}H NMR spectroscopy. Size exclusion chromatography (SEC) was used to determine a molecular weight of 10 kg/mol and a polydispersity of 1.18. A hydrosilation reaction[29,30] was employed to functionalize this polymer. The polymer (1.3 g) was placed inside a round-bottom flask with a stir bar. H_2PtCl_6 (ACS; Aldrich) was added under an argon atmosphere, and the flask was sealed with a rubber septum. Degassed benzene (50 mL; ACS; Aldrich) was distilled from calcium hydride (coarse granules; Aldrich) into the flask, and this was followed by the injection of 0.2 mL of $SiMeCl_3$ (99+%; Aldrich). The mixture was vigorously stirred overnight to react with impurities. $HSiMe_2Cl$ (98%; Aldrich) was purified over calcium hydride overnight, distilled the following day, and added to the polymer solution with a gas-tight syringe. The hydrosilation reaction was carried out at room temperature for 1 h and was continued in an oil bath at 45 °C overnight.

Another batch of living polybutadiene (90% 1,2-addition) was prepared with *sec*-butyllithium in a 150/1 ratio of [THF]/[Li] with a targeted molecular weight of 5 kg/mol. The hydrosilated compound was added to the living solution and allowed to react at room temperature for 3 days; this was followed by the addition of degassed isopropanol to ensure complete termination. The resulting product was a mixture of the desired highly branched polybutadiene and unreacted linear chains; the comb polymer had a 10.0 kg/mol backbone and an average of 62 branches of 5.5 kg/mol each according to SEC and light scattering (LS). This corresponded to 13 branches per 100 backbone carbon atoms. This polymer is denoted B90 because it is a branched polymer with 90% EE repeat units.

Catalytic Saturation

Linear Polybutadienes

The linear polybutadienes were saturated with either H_2 or D_2 at 500 psi and 70 °C over a $Pd/CaCO_3$ catalyst (5%; Strem) for 18 h with established techniques.[31] A Parr Instrument Co. 2-L high-pressure reactor was employed.

Highly Branched Polybutadiene

The branched polybutadiene was saturated in the presence of a Ni/Al coordination catalyst, which was found to be more efficient than the heterogeneous catalyst. Nickel 2-ethylhexanoate (78% in 2-ethylhexanoic acid, 10–15% Ni; Strem) was dissolved in cyclohexane, washed in distilled water twice, separated, and dried overnight in a vacuum oven at 110 °C. It was then redissolved in distilled cyclohexane, sealed, and purged with high-purity Ar for 30 min. The amount of catalyst employed was 0.4 g of Ni catalyst/g of polymer. Triethylaluminum (1.0 M in hexane; Aldrich) was added to the Ni catalyst in an inert atmosphere in a 3/1 molar ratio. An instantaneous color change from green to brown indicated the formation of the active Ni/Al coordination catalyst.

A cyclohexane solution of the branched polybutadiene (2–5% w/v) was sealed in a custom-built high-pressure reactor;[32] this was followed by injection of the catalyst solution with a gas-tight syringe. Hydrogen (or deuterium) was introduced and maintained at 500 psi while the solution was stirred at 70 °C for 48 h.

The catalyst was separated from the product by vigorous washing with 5% citric acid (of the same volume as the polymer solution) until the brownish polymer solution turned white. The solution was then allowed to phase-separate. After

Table II. Polymer Molecular Characteristics

Polymer	M_w[a], kg/mol	M_w/M_n[a]	ρ_H, g/cm^3 [b]	ρ_D, g/cm^3 [b]	n_D[c]	dn/dc[d]
L90A	220	1.02	0.8646	0.9129	3.02	0.132
L90	60	1.06	0.8643	0.9083	2.75	0.131
L83	60	1.01	0.8620	0.9042	2.64	0.135
L78	60	1.01	0.8624	0.9022	2.49	0.140
L73	55	1.01	0.8625	0.9054	2.68	0.143
L68	54	1.06	0.8618	0.9058	2.75	0.147
L55	65	1.02	0.8627	0.9053	2.66	0.156
B90	350	1.02	0.8685[e]	0.9006	2.00	0.134

[a] Based on SEC and LS.
[b] All densities measured at 25°C, with an uncertainty of ±0.0002.
[c] Average number of deuterons per C_4 repeat unit, with an uncertainty of ±0.03.
[d] Refractive index increment for polybutadiene in THF.
[e] This value includes a small contribution from the Si atoms at each graft junction (see text).

the organic phase passed through a packed basic alumina column, the saturated polymer was precipitated in a 3/1 methanol/isopropanol solution and vacuum-dried. Complete (i.e., >99%) saturation was confirmed by the disappearance of the characteristic olefinic resonances in solution ^{1}H NMR analysis for both the linear and branched polymers.

Fractionation

Fractionation of the desired saturated comb polymer from the unreacted short linear arms was accomplished in a toluene/methanol system at a 2–5% w/v concentration. The polymer was dissolved in toluene (ACS; Aldrich) at room temperature, and methanol (ACS; Aldrich) was added gradually until the solution became cloudy. After slowly heating until clear, the solution was poured into an insulated separatory funnel and set aside overnight. By the following day, the solution had phase-separated into two layers, with the bottom layer rich in the branched polymer. This procedure was repeated three to five times for the bottom layer until only one peak was detected by SEC.

Characterization

Weight-average molecular weights (M_w) and polydispersities [weight-average molecular weight/number-average molecular weight (M_w/M_n)] were determined by SEC with a multiangle light scattering detector (Wyatt Dawn) and refractive-index detector (Wyatt Optilab), with *dn/dc* determined from a series of diluted polymer solutions with the refractive-index detector. THF was employed as the mobile phase. The results are listed in Table 2. *dn/dc* decreased as the 1,2-content in the polybutadiene increased; this was consistent with an early report.[33]

^{1}H NMR spectroscopy was used to determine the 1,2-content of the backbone (67%) and arm precursor molecules (90%) of the branched polybutadiene and the various microstructured linear polybutadienes (55–90%) and to determine the level of product saturation (>99% in all cases).

Polymer densities were measured at 25 °C with a density gradient column with isopropanol/ethylene glycol as the suspending medium.[32] The density gradient column was calibrated with colored glass beads of known density. The average number of deuterium atoms per repeat unit was calculated with the density difference between the partially deuterated polymer and the corresponding hydrogenated polymer. Table 2 summarizes the molecular characteristics.

Sample Preparation

All mixtures were prepared by codissolution of the components in cyclohexane followed by precipitation in cold methanol, with subsequent drying *in vacuo* at room temperature (see Table 3 for the blend compositions). SANS samples were loaded between quartz disks separated by 1.2-mm aluminum spacers and then were sealed with a high-temperature adhesive. SANS samples were annealed at 100 °C for 72 h for the elimination of voids.

Table III. Blend Type, Compositions and Miscibility

Blend		ϕ[a]	Miscibility[b]
Isotopic Blends	dB90/B90 25/75	0.244	Yes
	dB90/B90 50/50	0.484	Yes
	dB90/B90 75/25	0.746	Yes
	dL90A/L90A	0.481	Yes
	dL90/L90	0.485	Yes
	dL83/L83	0.478	Yes
	dL78/L78	0.490	Yes
	dL73/L73	0.496	Yes
	dL68/L68	0.485	Yes
	dL55/L55	0.491	Yes
Comb/Linear Blends	dB90/L90 25/75	0.237	Yes
	dB90/L90 50/50	0.487	Yes
	dB90/L90 75/25	0.721	Yes
	dB90/L83	0.488	No
	dB90/L78	0.480	No
	dB90/L73	0.484	No
	dB90/L68	0.479	No
	dB90/L55	0.496	No
Linear/Linear Blends	dL90A/L83	0.494	Yes
	dL90A/L78	0.479	Yes
	dL90A/L73	0.480	No
	dL90A/L68	0.497	No
	dL90A/L55	0.485	No

[a] Volume composition of deuterated component.
[b] Forms one phase mixture at room temperature.

SANS

SANS experiments were conducted on the NIST/Exxon/University of Minnesota 30-m instrument (NG7) at the National Institute of Standards and Technology (Gaithersburg, MD) with a wavelength of $\lambda = 6$ Å with $\Delta\lambda/\lambda = 0.10$ and sample-to-detector distances of 7.5 and 15.3 m. All data were obtained at room temperature. Raw data were corrected for detector sensitivity and beam-blocked background detector counts and were normalized for sample transmission and sample thickness. Absolute calibration was accomplished with a Porasil B secondary standard.[34] The scattering results were averaged to produce one-dimensional absolute scattering intensity as a function of the magnitude of the scattering wavevector $q = (4\pi/\lambda)\sin(\theta/2)$, where θ is the scattering angle.

RESULTS

SANS Fitting

All of the pure saturated polymer samples produced predominantly incoherent scattering profiles. After subtraction of the incoherent component, which was taken to be the high-q asymptotic value, the coherent intensity was fitted to the polymer form factor described next.

The RPA equation for a two-component blend of monodisperse polymers was used to fit the SANS data:

$$I(q) = \frac{V^{-1}(\rho_1 - \rho_2)^2}{\frac{1}{\phi_1 S_1} + \frac{1}{(1-\phi_1)S_2} - 2\chi} \quad (1)$$

where V is the reference volume; ρ_i and ϕ_i are the scattering length density and volume fraction of component i, respectively; S_1 and S_2 are the single-chain form factors; and χ is the interaction parameter. We chose $V = 65$ cm^3/mol, which corresponds to one 4-carbon repeat unit. Casassa and Berry,[35] and subsequently Fredrickson and coworkers[24,25] derived the following comb polymer form factor:

$$S(q) = S_{BB}(q) + S_{AA}(q) + 2S_{AB}(q) \quad (2)$$

where S_{AB} is the correlation function between the backbone (B) and arm (A) repeat units. If we assume constant density and unperturbed Gaussian statistics for all backbone and branch chains, the three correlation functions appearing in eq 2 are given by

$$S_{BB}(q) = N_B^2 g(x_B)/N \quad (3)$$

$$S_{AA}(q) = nS_{AA1}(q) + S_{AA2}(q) \quad (4)$$

$$S_{AA1}(q) = N_A^2 g(x_A)/N \quad (5)$$

$$S_{AA2}(q) = \alpha N_B(\alpha N_B - 1)N_A^2 h(x_A)^2 g(x_B)/N \quad (6)$$

$$S_{AB}(q) = \alpha N_A N_B^2 h(x_A) g(x_B)/N \quad (7)$$

In these equations, N_B is the number of repeat units of the backbone, N_A is the number of repeat units of the arm, $S_{AA1}(q)$ is the partial structure factor between the repeat units on the same arm, and $S_{AA2}(q)$ is the partial structure factor between the repeat units on different arms. The number of branches per polymer is denoted n ($N = N_B + nN_A$), and α is the probability of a branch per backbone repeat unit. Other quantities appearing in these equations are

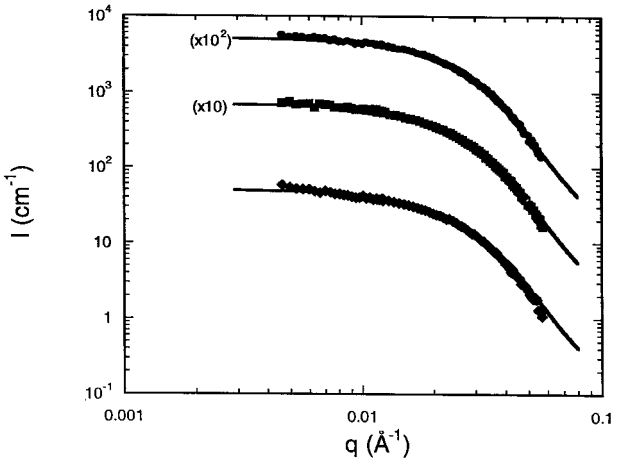

Figure 1. SANS results for (●) 25/75, (■) 50/50, and (♦) 75/25 dB90/B90 isotopic blends. The solid lines are fits with the branched polymer form factor.

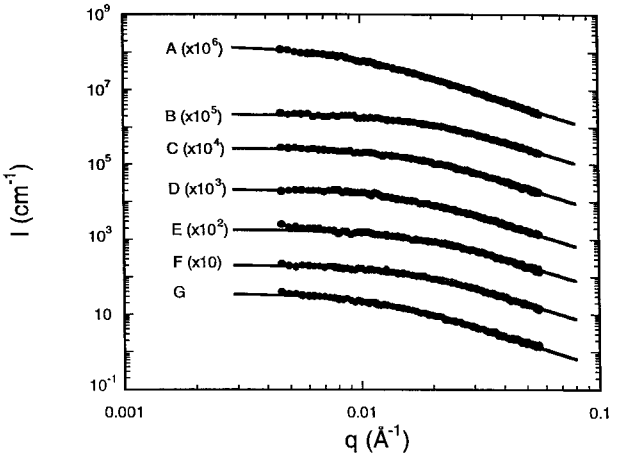

Figure 2. SANS results for (A) dL90A/L90A, (B) dL90/L90, (C) dL83/L83, (D) dL78/L78, (E) dL73/L73, (F) dL68/L68, and (G) dL55/L55 with 50/50 compositions. The solid lines are Debye function fits.

$$g(x) = 2(e^{-x} + x - 1)/x^2 \quad (8)$$

$$h(x) = (1 - e^{-x})/x \quad (9)$$

$$x_B = q^2 b^2 N_B/6 \quad (10)$$

$$x_A = q^2 b^2 N_A/6 \quad (11)$$

where b is the statistical segment length. For linear polymers, the form factor is simply $N_L g(x)$, where $g(x)$ is defined in eq 8 with $x = q^2 b^2 N_L/6$ and N_L is the degree of polymerization.

Isotopic Blends

SANS data from 25/75, 50/50, and 75/25 blends of dB90/B90 were fitted with the comb polymer form factor, as shown in Figure 1. The statistical segment length b and the χ parameter were the only fitting parameters. The predicted comb form factor[24] matched the results well, yielding $b_B = 7.9 \pm 0.5$ Å and $\chi = (0.3 \pm 1.0) \times 10^{-4}$ for all three blends. The resulting b_B and χ values were also in good agreement with previous measurements[26] for a 50/50 blend of a similar highly branched comb polymer of 750 kg/mol, where $b_B = 7.6 \pm 0.7$ Å and $\chi = (0.9 \pm 1.2) \times 10^{-4}$. The 50/50 isotopic blends of linear PE_{Exx} were evaluated similarly with the Debye function, as shown in Figure 2. All the statistical segment lengths and χ values extracted from these fits are listed in Table 4. The χ values were consistently very small (essentially zero within the uncertainty), as expected for these partially deuterated polyolefins.[36]

Comb/Linear Blends

The comb/linear blend series contained the deuterated branched polymer dB90 as the fixed component. The linear components varied in microstructure from 90 to 55% EE, with molecular weights that were approximately the same, about 60 kg/mol. Table 3 summarizes the information about the blend composition and miscibility. Starting with the miscible blends in which the components had the same 90% EE microstructure (i.e., dB90/L90 blends), we fitted the SANS data with the RPA equation with the linear and branched single-chain structure factors discussed

Table IV. Statistical Segment Length and Interaction Parameter for Isotopic Blends

Polymer	b[a], Å	$10^4\ \chi_{HD}$[a]
B90	7.9 ± 0.5	0.3 ± 1.0
L90A	5.8 ± 0.1	1.8 ± 1.4
L90	5.7 ± 0.2	1.4 ± 1.6
L83	6.0 ± 0.2	1.2 ± 1.3
L78	6.3 ± 0.2	1.1 ± 1.2
L73	6.5 ± 0.2	0.8 ± 1.2
L68	6.8 ± 0.2	1.2 ± 1.8
L55	7.2 ± 0.2	1.4 ± 1.8

[a] Determined by fitting SANS data using RPA equation for both b and χ_{HD}.

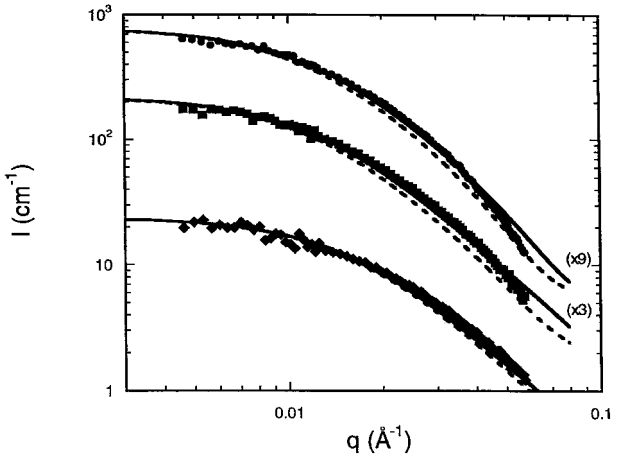

Figure 3. SANS results for (●) 25/75, (■) 50/50, and (♦) 75/25 dB90/L90A blends. The dashed curves represent the RPA fit for which χ was the only adjustable parameter. The solid line represents a fit for which both b_B and b_L were adjusted, with χ constant from the dashed line fits.

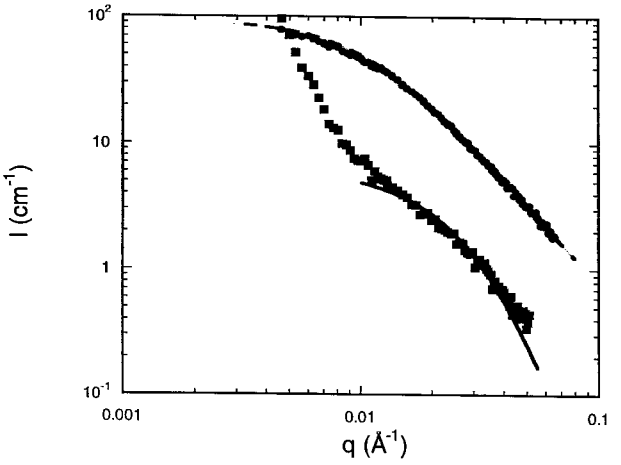

Figure 4. SANS results for (■) dB90/L83 and (●) dL90A/L83 blends with 50/50 compositions. The solid line is the Debye function fit for dL90A/L83, whereas the dashed line is an RPA fit assuming symmetric phase separation.

in the previous section. Figure 3 shows the scattering intensities as a function of q, along with the calculated fits. In the fit represented by the dashed line, χ was the only adjustable parameter, with the statistical segment lengths taken from the corresponding isotopic blend data. There were some deviations between the data and the calculated scattering intensities, particularly for $q > 0.01$ Å^{-1}. The resulting fitted χ values were $(7.2 \pm 1.2) \times 10^{-4}$, $(8.0 \pm 1.0) \times 10^{-4}$, and $(9.1 \pm 2.6) \times 10^{-4}$ for the 25/75, 50/50, and 75/25 compositions, respectively. For the fit shown by the solid line, these χ values were used as input, whereas the statistical segment lengths of the branched polymer and the linear polymer were varied to obtain the best fit to the actual data. This yielded $b_B' = 6.6$ Å and $b_L' = 5.7$ Å for the 25/75 composition, $b_B' = 5.1$ Å and $b_L' = 5.6$ Å for the 50/50 composition, and $b_B' = 5.7$ Å and $b_L' = 5.7$ Å for the 75/25 composition; the original values were $b_B = 7.9$ Å and $b_L = 5.7$ Å for the isotopic blends. The linear polymer statistical segment lengths were virtually unchanged, whereas the branched polymer statistical segment lengths were significantly reduced in all cases. The solid line fits were much improved compared with the dashed line fits and described the data quite well.

The other comb/linear blends were all immiscible, as shown by the SANS results shown in Figures 4–8. The solid squares in Figures 4–8 are the scattering intensities of the comb/linear blends dB90/L83, dB90/L78, dB90/L73, dB90/L68, and dB90/L55, respectively, as a function of q. All these mixtures displayed a strong increase in intensity as q was reduced below 0.01 Å^{-1}, with an approximate scaling of $I(q) \sim q^{-4}$. This is symptomatic of interfacial (Porod) scattering from a two-phase state. Moreover, the dB90/L83 and dB90/L78 blends had a high-q portion ($q > 0.01$ Å^{-1}) that could be modeled with the form of the RPA equations (the solid lines in Figs. 4 and 5, respectively). In these fits, we used two parameters, the χ parameter and the effective

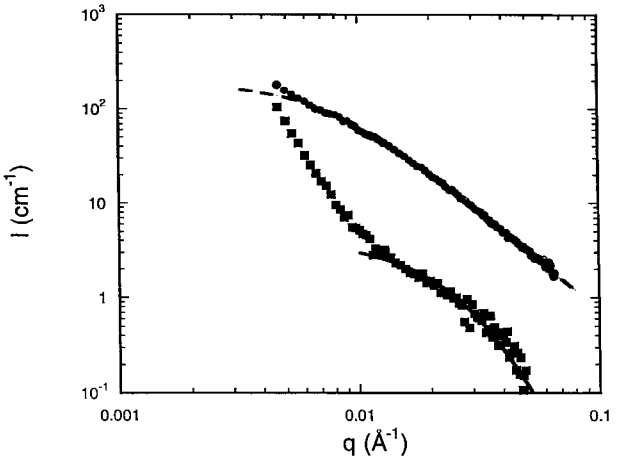

Figure 5. SANS results for (■) dB90/L78 and (●) dL90A/L78 blends with 50/50 compositions. The solid line is the Debye function fit for dL90A/L78, whereas the dashed line is an RPA fit assuming symmetric phase separation.

composition ϕ_{eff}. ϕ_{eff} was used as a fitting parameter because these blends were not spatially homogeneous. The original blend composition shown in Table 3 now becomes a gross concentration averaged over the entire blend, whereas the local concentration in the phase-separated domains will deviate significantly from the original concentration, depending on the degree of segregation. If the phase separation is symmetric (i.e., the concentration of comb polymer in comb-rich domains is the same as the concentration of linear polymer in linear-rich domains), we only need one ϕ_{eff}. The fitted ϕ_{eff} values were 0.019 and 0.009 for dB90/L83 and dB90/L78, whereas the fitted χ values were 0.0015 and 0.0044, respectively. The much reduced ϕ_{eff} value relative to the original values of 0.488 and 0.480 was consistent with the conclusion based on the low-q scattering that these two blends were well-segregated. The decreasing ϕ_{eff} values were also indicative of the increasing phase separation as the linear component changed from L83 to L78. A reduction in the EE content further reduced ϕ_{eff}, as illustrated in Figures 6–8 for blends dB90/L73, dB90/L68 and dB90/L55, respectively. In Figure 8, only Porod scattering is evident, consistent with nearly complete phase segregation, that is, $\phi_{eff} \rightarrow 0$.

Linear/Linear Blends

The linear/linear blend series had dL90A as the fixed component. The other components varied in microstructure from 83 to 55% EE. The five linear/linear blends also exhibited a range of scattering behavior; the scattering intensities are plotted as a function of q in Figures 4–8 as solid circles. Of the five blends, dL90A/L83 and dL90A/L78 were miscible (Figs. 4 and 5), whereas the other three blends phase-separated. We fit the data for dL90A/L83 and dL90A/L78 to the RPA equation with χ as the only fitting parameter, with statistical segment lengths from the isotopic blends. The fitted χ value increased from $(6.6 \pm 0.9) \times 10^{-4}$ to $(9.2 \pm 0.6) \times 10^{-4}$ with the decrease in the EE percentage. This was consistent with the observed phase separation for dL90A/L73, dL90A/L68, and dL90A/L55. In addition, the progressively decreasing intensities of these blends, as shown in Figures 6–8, indicated increasing segregation levels and coarsened grain sizes as the difference in microstructure increased.

DISCUSSION

For the linear/linear blends, we can anticipate the experimental results by employing the solubility parameter approach:[37]

$$\chi = \frac{V_{ref}}{RT}(\Delta\delta)^2 \tag{12}$$

where $\Delta\delta$ is the solubility parameter difference between the blend components. With $R = 8.314$ J/mol K, $T = 293$ K, and a repeat unit volume of

$$V_{ref} = 56 \text{ g/mol}/0.86 \text{ g/cm}^3 = 65 \text{ cm}^3/\text{mol} \tag{13}$$

χ becomes

$$\chi = 0.027(\Delta\delta)^2 \tag{14}$$

For a polymer blend, the critical χ and composition for the Flory–Huggins theory are given by

$$\chi_c = \frac{(N_1^{1/2} + N_2^{1/2})^2}{2N_1N_2} \tag{15}$$

$$\phi_c = \frac{N_2^{1/2}}{N_1^{1/2} + N_2^{1/2}} \tag{16}$$

For example, for dL90A/L83 the fixed linear component dL90A had a molecular weight of 220 kg/mol ($N_1 = 4000$) with a microstructure of 90% EE, whereas the second component L83 had a molecular weight of 60 kg/mol ($N_2 = 1070$) with 83% EE. From these values, we can extract $(\Delta\delta)_c = 0.20$ with eq 15 and $\phi_c = 0.34$, with eq 16. Similarly, the calculated $(\Delta\delta)_c$ and ϕ_c values for all these linear/linear blends are shown in Table 5.

However, these blends were not generally at the critical composition. For these upper critical solution temperature blend systems, the calculated $\Delta\delta_c$ represents the minimum required for phase separation at the critical composition. At another composition, $\phi \approx 0.5$, the required $\Delta\delta_{min}$ for phase separation should be somewhat greater than $\Delta\delta_c$. From the Flory–Huggins theory stability limit,

$$\frac{1}{\phi_1N_1} + \frac{1}{\phi_2N_2} - 2\chi_S = 0 \tag{17}$$

Table V. Comparison of Solubility Parameter Predictions and Experiments

Blends	$\Delta\delta_c$, $MPa^{1/2}$	ϕ_c	$\Delta\delta_{min}$, $MPa^{1/2}$	$\Delta\delta$, $MPa^{1/2}$	Predictions	Experimental Results
dL90A/L83	0.20	0.34	0.21	0.16 ± 0.01	Miscible	Miscible
dL90A/L78	0.20	0.34	0.21	0.27 ± 0.02	Immiscible	Miscible
dL90A/L73	0.21	0.33	0.22	0.38 ± 0.02	Immiscible	Immiscible
dL90A/L68	0.21	0.33	0.22	0.48 ± 0.02	Immiscible	Immiscible
dL90A/L55	0.20	0.35	0.21	0.75 ± 0.03	Immiscible	Immiscible

we estimate $\Delta\delta_{min}$, which is also listed in Table 5. $\Delta\delta_{min}$ and $\Delta\delta_c$ are sufficiently close that we ignore these differences. $\Delta\delta$ was estimated for these blends with an empirical equation provided by Graessley et al.:[11]

$$\delta(y_1) - \delta(y_2) = -(\delta_{H00} - \delta_{H100})(1 - \gamma + 2\gamma\bar{y})\Delta y \quad (18)$$

$$\bar{y} = (y_1 + y_2)/2 \quad (19)$$

$$\Delta y = y_2 - y_1 \quad (20)$$

where y is the percentage of EE units, H00 refers to pure PE, H100 refers to pure PEE, and γ is an empirical (fitted) constant. Graessley et al. gave $\delta_{H00} - \delta_{H100} = 1.90 \pm 0.03$ and $\gamma = 0.27 \pm 0.06$ at 27 °C. Using these numbers, we determined the $\Delta\delta$ values shown in Table 5. When $\Delta\delta < \Delta\delta_c$ (or $\Delta\delta_{min}$), the blend should be miscible, whereas $\Delta\delta \geq \Delta\delta_c$ (or $\Delta\delta_{min}$) anticipates an immiscible blend according to the solubility parameter formalism. Table 5 summarizes the results for all the linear/linear blends.

As can be seen, the solubility parameter predictions agree well with the experimental results, except for blend dL90A/L78. The solubility parameter approach predicts immiscibility, whereas the experiment shows miscibility. However, the solubility parameter prediction must be considered a rough estimate. The $\Delta\delta$ values are not precise because they are calculated from empirical values with relatively large uncertainties at a different, though close, temperature (27 °C). The resulting $\Delta\delta$ values have 4–6% error, as shown in Table 5. Furthermore, for dL90A/L78, the values for $\Delta\delta_c$, $\Delta\delta_{min}$, and $\Delta\delta$ are similar, differing only slightly in the last significant figure. It is likely that the calculation is not accurate enough, and this may explain the miscibility of dL90A/L78.

The dL90A polymer was miscible with both L83 and L77. However, the branched polymer dB90, which had the same microstructure (90% EE) as dL90A and only a slightly higher molecular weight (350 kg/mol vs. 220 kg/mol), was immiscible with both L83 and L77. Furthermore, although it was miscible with L90, the blend also had relatively large χ values for all three compositions examined. These results all underscore the importance of the architectural difference between branched and linear polymers. This architectural contribution to χ is so significant that it greatly reduces the miscibility window of PE_{Exx} polymers with different microstructure as we switch dL90A to dB90. In terms of the field theory predictions,[24] these data show that for these blends, χ_ϵ arising from the long-range architectural interactions is comparable in magnitude to χ_o, which is proportional to the heat of mixing, because of differences in the percentage of EE repeat units.

The architectural difference between branched and linear polymers is also evident in the measured statistical segment lengths. Figure 9 shows the experimentally determined statistical segment lengths for various microstructure linear PE_{Exx}'s, along with literature values.[9,38] A line can be fit to these values, showing an excellent correlation. However, previously[26] we reported a significantly larger statistical segment length, 7.9 ± 0.5 Å, for B90 than for linear polymers of the same microstructure (L90A and L90), suggesting that the branches were highly stretched in the undiluted melt state. Because of chemical connectivity and spatial restrictions (i.e., constant density), these molecules cannot pack as unperturbed Gaussian chains. To fill space uniformly, some chain stretching, which is entropically unfavorable, is inevitable. In addition, these constraints can distort the chain conformations inhomogeneously, with the most severe stretching presum-

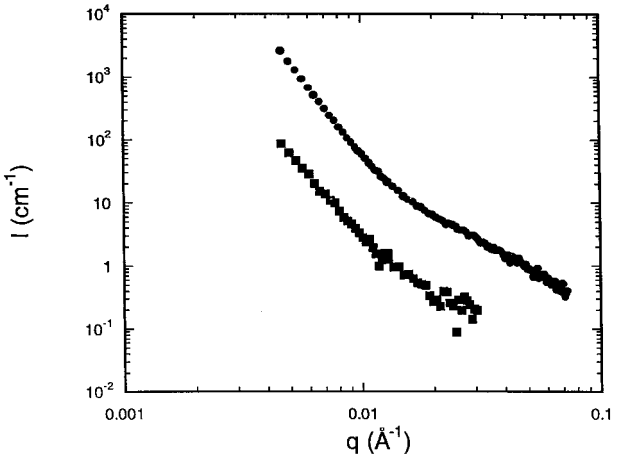

Figure 6. SANS results for (■) dB90/L73 and (●) dL90A/L73 blends with 50/50 compositions.

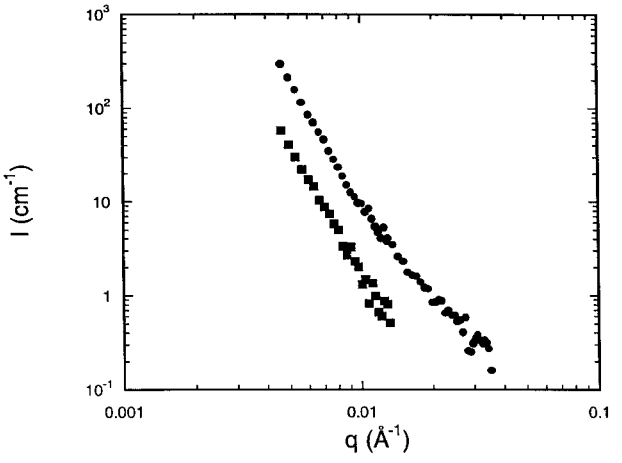

Figure 7. SANS results for (■) dB90/L68 and (●) dL90A/L68 blends with 50/50 compositions.

ably occurring near the backbone.[39] These greater statistical segment length values also reflect a departure from the assumptions in the RPA calculation.

The addition of conformationally less restricted linear polymer may provide energetically favorable degrees of freedom that assist in alleviating the packing constraints existing in the heavily branched polymer, thereby reducing the statistical segment length of the branched polymer. The heavily branched polymer seems to be less stretched in its blend with linear polymers than in its own melt, as seen in Figure 3. Holding the statistical segment lengths constant (with the extrapolated values from isotopic blends) while fitting χ gave a less satisfactory fit, especially at q > 0.01 Å^{-1}. Because χ only influences the low-q part of the scattering, we allowed the statistical segment lengths of the components to vary while holding χ constant; the resulting fits were much improved and agreed very well with experimental data. This resulted in an unchanged b_L' and much reduced b_B'. The new fitted b_B' values were 6.6, 5.1, and 5.7 Å for 25/75, 50/50, and 75/25 dB90/L90, respectively. The largest reduction occurred at the 50/50 composition. The b_B' value for the 75/25 blend was lower than that for the 25/75 blend. This is an indication that it is thermodynamically more favorable to mix a small amount of a linear component into a branched melt than the reverse, as the theory predicts.[24,25] Although this argument suggests a favorable conformational contribution for mixing heavily branched and linear polyolefins, implying a negative contribution to χ, the mixing is likely to be nonrandom. This is because unperturbed linear PE_{Exx} cannot be randomly interchanged with branched PE_{Exx}. A positive excess free energy of mixing will arise from the nonrandom mixing and conformational rearrangements that facilitate mixing. We infer that the high χ values for the comb/linear blends result from this packing frustration.

The convergence of the scattering intensities in the phase-separated comb/linear and linear/linear blends in moving from Figures 6 to 8 reinforce these deductions regarding the effect of branching on miscibility. In the limit of greatest thermodynamic incompatibility (Fig. 8), virtually pure component phases coexist, and I(q) accordingly contains solely Porod scattering ($I \sim q^{-4}$); that is, Debye scattering is not evident. Therefore, the absolute scattering

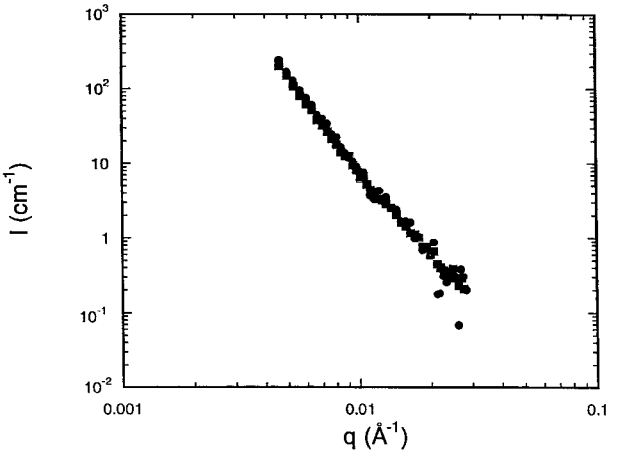

Figure 8. SANS results for (■) dB90/L55 and (●) dL90A/L55 blends with 50/50 compositions.

intensity will be determined by the Porod constant, which depends on the contrast factor and the domain size (interfacial area).[40] Remarkably, as the incompatibility increased, the linear/linear and linear/branched phase-separated blends yielded nearly indistinguishable Porod scattering. After accounting for differences in contrast factors (there were only 2.00 deuterons per repeat unit for the comb polymer dB90 but 3.02 deuterons per repeat unit for the linear polymer dL90A; Table 2), we can conclude that the growth of the two-phase structure is arrested at roughly comparable scales, $D_{dB90} \approx 16\ \mu m$ and $D_{dL90A} \approx 30\ \mu m$, where D is the Porod diameter with a spherical geometry assumed.

Two other possible contributing factors to χ must be addressed. A small contribution to χ may be associated with isotope effects.[36] The measured χ_{HD} values for the linear isotopic blends were, on average, 1.3×10^{-4} (Table 4), barely resolved above the statistical uncertainties of the measurements. In contrast, the interaction parameters measured from all the miscible blends were significantly greater (Table 6). Consequently, we conclude that although the isotope effect may influence the results shown here, it is at most a minor contribution.

The second factor concerns the Si atom in the branched polymer. The measured density of B90 was 0.8685 g/cm^3, somewhat higher than the densities of L90A and L90, which were 0.8646 and 0.8643 g/cm^3, respectively. However, with the additional Si atoms at the branching points taken into consideration, the corrected density was 0.8642 g/cm^3, which agreed very well with L90A and L90. Although these additional C—Si bonds had an effect on density, their contribution to χ was estimated to be entirely negligible, about 10^{-7}, on the basis of group additivity calculations.[41]

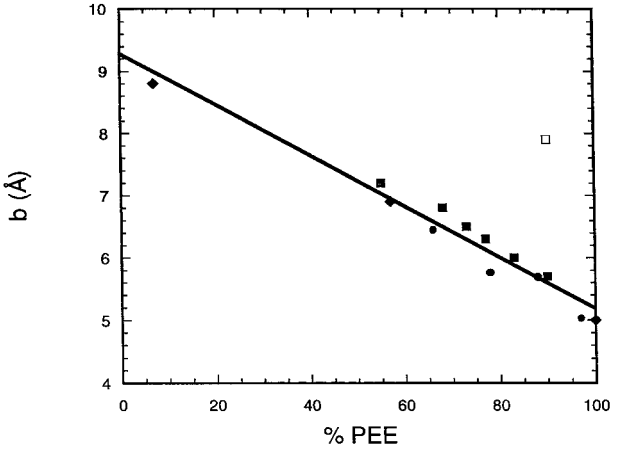

Figure 9. Statistical segment lengths for various different microstructured PEE*xx*. (■) Our linear data, (●) Graessley et al.'s data,[9] and (♦) Bates et al.'s data[36] were fitted with the solid line with linear regression. The open square corresponds to the branched B90 data.

Table VI. Interaction Parameters for Miscible Blends

Blend Composition	$10^4\ \chi^a$
dB90/L90 25/75	7.2 ± 1.2
dB90/L90 50/50	8.0 ± 1.0
dB90/L90 75/25	9.1 ± 2.6
dL90A/L83	6.6 ± 0.9
dL90A/L78	9.2 ± 1.1

[a] χ is the only fitting parameter.

CONCLUSIONS

SANS experiments established that a 220 kg/mol linear PE_{E90} formed single-phase 50/50 melt mixtures with linear 60 kg/mol PE_{E83} and PE_{E78} but phase-separated from PE_{E73}, PE_{E68}, and PE_{E55}. However, a 350 kg/mol PE_{E90} comb polymer phase-separated from all these linear PE_{Exx} random copolymers. Although it was miscible with linear PE_{E90}, the χ values were relatively large. These results demonstrate that two factors are operative in determining phase behavior in polyolefin blends. Differences in short-chain branching produce enthalpic contributions, whereas long-chain branching results in an excess entropy of mixing.[42] Both effects increase the magnitude of the Flory–Huggins χ parameter and either can induce phase separation between linear and branched polyolefins.

The authors are grateful to the U.S. Department of Energy for funding under contract number DE-AC05-960R22464 with Lockheed Martin Energy Research Corp.

REFERENCES AND NOTES

1. Agmalian, M.; Alamo, R. G.; Kim, M. H.; Londono, J. D.; Mandelkern, L.; Wignall, G. D. Macromolecules 1999, 32, 3093.
2. Alamo, R. G.; Londono, J. D.; Mandelkern, L.; Stehling, F. C.; Wignall, G. D. Macromolecules 1994, 27, 411.

3. Hill, M. J.; Morgan, R. L.; Barham P. J. Polymer 1997, 38, 3003.
4. Hill, M. J.; Barham, P. J. Polymer 1997, 38, 5595.
5. Thomas, D.; Williamson, J.; Hill, M. J.; Barham, P. J. Polymer 1993, 34, 4919.
6. Tsukahara, Y.; Inoue, J.; Ohta, Y.; Kohjiya, S. Polymer 1994, 35, 5785.
7. Greenberg, C. C.; Foster, M. D.; Turner, C. M.; Corona-Galvan, S.; Cloutet, E.; Butler, P. D.; Hammouda, B.; Quirk, R. P. Polymer 1999, 40, 4713.
8. Greenberg, C. C.; Foster, M. D.; Turner, C. M.; Corona-Galvan, S.; Cloutet, E.; Quirk, R. P.; Butler, P. D.; Hawker, C. J Polym Sci Part B: Polym Phys 2001, 39, 2549.
9. Graessley, W. W.; Krishnamoorti, R.; Reichart, G. C.; Balsara, N. P.; Fetters, L. J.; Lohse, D. J. Macromolecules 1995, 28, 1260.
10. Krishnamoorti, R.; Graessley, W. W.; Fetters, L. J.; Garner, R. T.; Lohse, D. J. Macromolecules 1995, 28, 1252.
11. Graessley, W. W.; Krishnamoorti, R.; Balsara, N. P.; Butera, R. J.; Fetters, L. J.; Lohse, D. J.; Schulz, D. N.; Sissano, J. A. Macromolecules 1994, 27, 3896.
12. Krishnamoorti, R.; Graessley, W. W.; Balsara, N. P.; Lohse, D. J. Macromolecules 1994, 27, 3073.
13. Graessley, W. W.; Krishnamoorti, R.; Balsara, N. P.; Fetters, L. J.; Lohse, D. J.; Schulz, D. N.; Sissano, J. A. Macromolecules 1994, 27, 2574.
14. Dudowicz, J.; Freed, K. F. Macromolecules 1996, 29, 8960.
15. Freed, K. F.; Dudowicz, J. Macromolecules 1996, 29, 625.
16. Dudowicz, J.; Freed, K. F. Macromolecules 1991, 24, 5076.
17. Dudowicz, J.; Freed, M. S.; Freed, K. F. Macromolecules 1991, 24, 5096.
18. Schweizer, K. S.; Curro, J. G. Phys Rev Lett 1988, 60, 809.
19. Curro, J. G.; Schweizer, K. S. J Chem Phys 1988, 88, 7242.
20. Schweizer, K. S.; Curro, J. G. J Chem Phys 1989, 91, 5059.
21. Bates, F. S.; Schulz, M. F.; Rosedale, J. H.; Almdal, K. Macromolecules 1992, 25, 5547.
22. Bates, F. S.; Fredrickson, G. H. Macromolecules 1994, 27, 1065.
23. Bates, F. S.; Schulz, M. F.; Khandpur, A. K.; Förster, S.; Rosedale, J. H.; Almdal, K.; Mortensen, K. Faraday Discuss 1994, 98, 7.
24. Fredrickson, G. H.; Liu, A. J.; Bates, F. S. Macromolecules 1994, 27, 2503.
25. Fredrickson, G. H.; Liu, A. J. J Polym Sci Part B: Polym Phys 1995, 33, 1203.
26. Chen, Y. Y.; Lodge, T. P.; Bates, F. S. J Polym Sci Part B: Polym Phys 2000, 38, 2965.
27. Hillmyer, M. A.; Bates, F. S. Macromolecules 1996, 29, 6994.
28. Ndoni, S.; Papadakis, C. M.; Bates, F. S.; Almdal, K. Rev Sci Instrum 1995, 66, 1090.
29. Iraqi, S.; Seth, S.; Vincent, C. A.; Cole-Hamilton, D. J.; Watkinson, M. D.; Graham, I. M.; Jeffery, D. J Mater Chem 1992, 2, 1057.
30. Hadijichristidis, N. J Polym Sci Part A: Polym Chem 1999, 37, 857.
31. Weimann, P. A.; Jones, T. D.; Hillmyer, M. A.; Bates, F. S.; Londono, J. D.; Melnichenko, Y.; Wignall, G. D.; Almdal, K. Macromolecules 1997, 30, 3650.
32. Gehlsen, M. D. Ph.D. Thesis, University of Minnesota, 1994.
33. Chen, X.; Xu, Z.; Hadjichristidis, N.; Fetters, L. J.; Carella, J.; Graessley, W. W. J Polym Sci Polym Phys Ed 1984, 22, 777.
34. Wignall, G. D.; Bates, F. S. J Appl Crystallogr 1988, 20, 28.
35. Casassa, E. F.; Berry, G. C. J Polym Sci Part A-2: Polym Phys 1966, 4, 881.
36. Bates, F. S.; Fetters, L. J.; Wignall, G. D. Macromolecules 1988, 21, 1086.
37. Although the theory of Fredrickson and coworkers[24,25] accounts for all types of chain branching, the necessity of employing a short wavelength cutoff introduces uncertainty in the limit of short branches. Graessley and coworkers[9–13] showed convincingly that enthalpic contributions play a significant, perhaps dominant, role in linear polyolefin blend thermodynamics. Because we have no basis for mixing these entropic and enthalpic treatments, we have opted to adopt the latter in dealing with our linear/linear mixtures.
38. Bates, F. S.; Schulz, M. F.; Rosedale, J. H.; Almdal, K. Macromolecules 1992, 25, 5547.
39. Daoud, M.; Cotton, J. P. J Phys (Paris) 1982, 43, 531.
40. Higgins, J. S.; Benoit, H. C. Polymers and Neutron Scattering; Oxford University Press: New York, 1994.
41. We estimate the C—Si bond contribution to the solubility parameter to be $\Delta\delta \cong 0.09 - 0.11$ (cal/cm)$^{1/2}$, which translates into an interaction parameter contribution of $\Delta\chi \cong 10^{-7}$ with the solubility parameter formalism.
42. We performed temperature studies on two miscible PE_{E90} blends. In these blends, both components have 90% EE repeat units; one is a linear polymer of 60 kg/mol (L90 in this article), and the other is a branched comb of 750 kg/mol. The two blends differ in composition: one blend has 7% branched comb, and the other has 25% of branched comb. We found that χ is nearly independent of temperature from 25 to 250 °C. χ changed from $(6.6 \pm 3.4) \times 10^{-4}$ at 25 °C to $(5.2 \pm 3.7) \times 10^{-4}$ at 250 °C for the 7/93 blend and from $(5.0 \pm 1.6) \times 10^{-4}$ at 25 °C to $(4.3 \pm 1.6) \times 10^{-4}$ at 210 °C for the 25/75 blend. This is consistent with the entropic origin of χ arising from long-chain branching.